FINAL REPORT

on

# INVESTIGATION OF FAILED FIELD ANCHOR HEADS HV016 AND HV038 FROM THE J. M. FARLEY NUCLEAR POWER PLANT UNIT 2 CONTAINMENT

to

INRYCO, INCORPORATED

April 9, 1985

by

T. P. Groeneveld

BATTELLE
Columbus Laboratories
505 King Avenue
Columbus, Ohio 43201

TABLE OF CONTENTS

# INVESTIGATION OF FAILED FIELD ANCHOR HEADS HV016 AND HV038 FROM THE J. M. FARLEY NUCLEAR POWER PLANT UNIT 2 CONTAINMENT

by

T. P, Groeneveld

## INTRODUCTION

On January 27, 1985, at the Joseph M. Farley Nuclear Power Plant operated by Alabama Power Company in Dolton, Alabama, Field Anchor Head HV016 from Tendon V17 in the Unit 2 containment was discovered to have failed. The failed anchor head was discovered during inspection of the containment posttensioning system while Unit 2 was shut down for refueling. On January 30, 1985, Field Anchor Head HV038 (from Tendon V21) was found to have failed also. The exact time of failure of those two field anchor heads was not known. Both had been in service since 1977, and the post-tensioning system was last inspected during June, 1983. At that time, all of the anchor heads inspected were found to be intact.

The two failed field anchor heads were part of the posttensioning system for the Unit 2 reactor containment. Both were machined from 10-inch-diameter hot-rolled-and-annealed steel rounds produced in accordance with the requirements set forth in ASTM A322 for Grade 4140/4142 alloy steel. Both anchor heads reportedly were fabricated from rounds produced from the same heat of steel (Republic Steel Company Heat No. 6061524), which was produced in 1973. In addition, both failed anchor heads were heat treated in the same lot by Downey Steel Treating Company, Downey, California, in accordance with Military Specification MIL-H6875 to a hardness of 40 to 44 Rockwell C ($R_C$).

The field anchor heads are 9.375 inches in diameter by 4 inches high. One hundred and seventy 0.257-in. diameter holes are drilled longitudinally through the central region of the anchor heads forming a honeycomb region. Cold-drawn-steel tendon wires (ASTM A421) pass through those holes and are cold headed during installation of the posttensioning

system. The field anchor heads are then pulled away from the bearing plate by jacks so as to stress the tendons, and ASTM A36 steel shims are inserted between the anchor head and the bearing plate when the proper tendon stress level is reached. After tensioning, grease covers are placed over the anchor heads, and corrosion-protection grease (Visco O 2090P) is pumped into the system (the field anchor grease cans, tendon conduit, and the shop anchor grease cans). At the Farley Plant, the grease covers and the tendon conduit were made of galvanized steel.

When the grease covers of both of the failed anchor heads were removed and examined subsequently, water was found in the grease. Analyses of the grease and water were performed by Inland Steel Company and Suburban Laboratories, Incorporated. In addition, flakes of zinc were found in the grease.

The failure of Field Anchor Head HV016 resulted in six major pie-shaped fractured pieces and numerous other smaller fragments. Two of the major pie-shaped pieces, identified as Pieces 4 and 5, were provided to Battelle's Columbus Laboratories for this investigation. The failure of Field Anchor Head HV038 produced two major pieces, with the fracture occurring essentially along a diameter of the anchor head. The plane of the major fracture was at an angle of approximately 30 degrees to the shim-stack gap. In addition, another crack had occurred through a portion of one of the broken halves, and a small fragment had broken out of the honeycomb region. Anchor Head HV038 was inspected at Inland Steel on February 18, 1985, by Inland Steel Metallurgical Laboratory personnel, Mr. G. Schmidt of Bechtel Corporation, Mr. H. Presswalla of INRYCO, and Mr. T. Groeneveld of Battelle. Following that inspection, one of the sections that represented approximately one-half of the failed anchor and the fragment that broke away from the honeycomb region were provided to Battelle for this study. The other half of the failed anchor, which contained the second major crack, was kept by Inland Steel for evaluation.

This report describes the metallurgical studies conducted at Battelle on Field Anchor Heads HV016 and HV038 to establish the most probable cause(s) of their failure.

## SUMMARY

The information obtained from the metallurgical evaluation of failed Anchor Heads HV016 and HV038 has shown that the most probable cause of their failure was hydrogen-stress cracking. The primary reasons for that conclusion were as follows:

(1) The fracture mode at the suspected origins and some other regions on the fracture surfaces was intergranular fracture.
(2) The anchor heads were heat treated to hardnesses in the range from 40 to 44 Rockwell C.
(3) The anchor heads were subjected to high stresses with tensile components during service.
(4) Water was present in the grease cans surrounding the anchor heads, and particles of zinc were entrained in the grease. In addition, zinc was detected on the fracture surfaces and the surfaces of the tendon holes.
(5) The failures occurred after the posttensioning system had been in service between 6 and 7 years.
(6) The absence of intergranular fracture on the fracture surfaces of the tensile and impact specimens tested in the laboratory indicated that the anchor heads were not embrittled by mechanisms that can result in intergranular fracture under purely mechanical loading, such as temper embrittlement or tempered-martensite embrittlement.
(7) Corrosion products usually associated with stress-corrosion cracking were not present on the fracture surfaces of the failed anchor heads.
(8) The absence of heat-treating scale on the fracture surfaces showed that quench cracks were not present in the suspected origin regions of the failures.

It is well established that low-alloy steels heat treated to hardnesses in a range that includes the 40 to 44 $R_C$ range of the anchor heads are susceptible to hydrogen-stress cracking when they are subjected to applied tensile stresses of suitable magnitude and either contain atomic hydrogen absorbed during prior processing or are placed in environments from which they can absorb atomic hydrogen during service. The high stresses in the anchor heads that result from the loading of the tendons would be sufficient to cause failure if the steels contain atomic hydrogen or absorb atomic hydrogen during service. The presence of water and zinc particles in the immediate vicinity of the anchor heads most likely was the source of the atomic hydrogen. Since zinc is electrochemically anodic to steel, it will preferentially corrode and thereby cathodically protect the steel if moisture is present. As a result of that cathodic protection, atomic hydrogen will be generated at the surface of the steel, and some of that hydrogen will be absorbed by the stressed steel, thus resulting in hydrogen-stress cracking after some period of time during which the cracks initiate and grow. When the hydrogen-stress cracks have grown to a critical size, which is a function of the toughness of the steel, its strength, and the applied stress level, the remaining section will fail rapidly by overstress failure.

The steel used to fabricate the anchor heads essentially met the chemical-composition requirements of ASTM A322, Grade 4140/4142, steel and the hardness requirements specified for the anchor heads. The minor deviation in average carbon content of the steel from Anchor Head HV038 was not responsible for its failure. The steel from both anchor heads was relatively dirty with respect to sulfide inclusions, a condition that contributed to lower ductility and impact properties in the transverse direction. However, that condition was not the cause of the cracking in the anchor heads.

To prevent similar failures of anchor heads in the future, steps should be taken to prevent water from contacting the surfaces of the steel. Those steps should include thoroughly coating the anchor-head surfaces

with corrosion-prevention grease and eliminating the source(s) of water in the posttensioning system. In addition, the design of the post-tensioning system should be reviewed, and consideration should be given to modifications that would permit the anchor heads to be made of a lower strength steel that will be less susceptible to hydrogen-stress cracking and other environmentally induced failure mechanisms.

## METALLURGICAL STUDIES

### Chemical Composition

A section from Piece 4 of Anchor Head HV016 and two sections, one from near the outer cylindrical surface and one from near the tendon holes, from Anchor Head HV038 were used to determine the chemical compositions of the steels using spectrographic-analysis techniques. The results of those analyses are listed in Table 1, along with the product-check-analysis range for ASTM A322, Grade 4140/4142, steel.

The results of those analyses indicated that the chemical compositions, except for the carbon content of the steel from HV038, were within the allowable limits for product analyses for ASTM A322, Grade 4140/4142, steel. For the steel from Anchor Head HV038, the average carbon content was 0.48 percent, or 0.01 percent above the maximum allowable amount. The sulfur content of the steel from both anchor heads was somewhat high, but well within the specified range. The aluminum content indicates that the heat of steel was aluminum killed. The levels of the other residual elements were low.

### Tensile Properties

The tensile properties of the steel from both anchor heads were determined with both longitudinal and transverse round tensile specimens. The axes of the longitudinal specimens were parallel to the axes of the cylindrical anchor heads and the axes of the transverse specimens were 90 degrees to axes of the anchor heads, or parallel to the circular faces of the

TABLE 1. RESULTS OF CHEMICAL ANALYSES OF SAMPLES FROM ANCHOR HEADS HV016 AND HV038

| Element | Chemical Composition, weight percent | | |
|---|---|---|---|
| | Sample HV016[a] | Sample HV038[a] | ASTM A322, Grade 4140/4142, Product-Analysis Range |
| C | 0.43 | 0.48[b] | 0.36/0.47 |
| Mn | 0.98 | 0.96 | 0.69/1.04 |
| P | 0.012 | 0.011 | 0.040 max |
| S | 0.026 | 0.023 | 0.045 max |
| Si | 0.22 | 0.23 | 0.13/0.37 |
| Cr | 1.02 | 1.09 | 0.75/1.15 |
| Mo | 0.21 | 0.21 | 0.13/0.27 |
| Cu | 0.094 | 0.12 | 0.35 max |
| Ni | 0.13 | 0.14 | 0.25 max |
| Al | 0.013 | 0.014 | -- |
| Sn | <0.005 | 0.009 | -- |
| Sb | <0.005 | <0.001 | -- |
| As | ND[c] | <0.005 | |
| V | <0.001 | <0.01 | -- |
| Co | <0.05 | <0.10 | -- |
| Cb | <0.01 | <0.01 | -- |
| Pb | <0.001 | 0.0002 | -- |
| Zr | <0.01 | <0.01 | -- |
| Ti | <0.01 | <0.01 | -- |
| W | <0.05 | <0.05 | -- |
| B | <0.0005 | <0.0005 | -- |

(a) Spectrographic analyses, average of two determinations per element.

(b) The individual carbon contents for the two analyses were 0.46 and 0.50; the higher carbon content was measured in the sample near the tendon-hole region.

(c) ND = not determined.

anchor heads. Because of the limited sizes of the two sections from Anchor Head HV016 received for this study, the tensile specimens from it were limited to a 0.250-inch-diameter reduced section and a 1-inch gage length. The specimens from Anchor Head HV038 had a 0.5-inch-diameter reduced section and a 2-inch gage length. Duplicate specimens of each orientation from each anchor head were tested. The tensile properties of the steels from the two anchor heads are listed in Table 2.

The results of the tensile tests showed that the average ultimate tensile strength of the steel from both anchor heads was about 200 ksi and that the average yield strength ranged from 181 to 186 ksi. There was relatively little difference in the strength properties among the specimens from the two anchor heads or for the specimens from the two orientations. Similarly, there were no substantial differences in the ductilities of the steels from the two anchor heads, although the ductility of the steel from Anchor Head HV038 was somewhat lower than that of the steel from Anchor Head HV016. However, as would be expected, the ductilities measured with the transverse specimens from each anchor head were substantially lower than those obtained with the longitudinal specimens.

## Impact Properties

The impact properties of the steel from both anchor heads were measured at room temperature and boiling-water temperature using full-size Charpy V-notch specimens machined from blanks removed from each anchor head in both the longitudinal and transverse directions. The impact properties obtained are listed in Table 3.

The results listed in Table 3 show that the impact properties of the specimens from both anchor heads were similar and that the energy absorbed by the transverse specimens was approximately one-half of that of longitudinal specimens. However, the values measured are considered reasonable for this grade of steel heat treated to the 200-ksi ultimate-tensile-strength level. All of the impact specimens tested at room

TABLE 2. TENSILE PROPERTIES OF ASTM A322, GRADE 4140/4142, STEEL FROM ANCHOR HEADS HV016 AND HV038

| Specimen Number | Specimen Orientation[a] | | Ultimate Tensile Strength, ksi | Yield Strength (0.2% Offset), ksi | YS/UTS | Elongation, percent in 4D | Reduction in Area, percent |
|---|---|---|---|---|---|---|---|
| | | | Anchor Head HV016[b] | | | | |
| 5-1 | L | | 203.3 | 186.1 | 0.92 | 13 | 47.4 |
| 5-2 | L | | 199.0 | 181.1 | 0.91 | 12 | 47.0 |
| | | Average | 201.2 | 183.6 | 0.92 | 12.5 | 47.2 |
| 4-1 | T | | 197.4 | 177.6 | 0.90 | 8.5 | 23.6 |
| 4-2 | T | | 201.4 | 184.4 | 0.92 | 7.5 | 16.2 |
| | | Average | 199.4 | 181.0 | 0.91 | 8.0 | 19.9 |
| | | | Anchor Head HV038[c] | | | | |
| 1 | L | | 198.8 | 183.0 | 0.92 | 11 | 44.4 |
| 2 | L | | 201.4 | 185.1 | 0.92 | 12 | 46.5 |
| | | Average | 200.1 | 184.1 | 0.92 | 11.5 | 45.5 |
| 3 | T | | 198.0 | 179.1 | 0.90 | 6 | 17.6 |
| 4 | T | | 207.8 | 193.3 | 0.93 | 6.5 | 12.3 |
| | | Average | 202.9 | 186.2 | 0.92 | 6.5 | 15.0 |

(a) L-specimen axis parallel to the axis of the cylindrical anchor head.
T-specimen axis parallel to the circular faces of the anchor head and approximately normal to a diameter.

(b) Determined with round tensile specimens with 0.250-inch-diameter reduced sections.

(c) Determined with round tensile specimens with 0.500-inch-diameter reduced sections.

TABLE 3. CHARPY-V-NOTCH-SPECIMEN IMPACT PROPERTIES OF THE STEELS FROM ANCHOR HEADS HV016 AND HV038

| Specimen Number | Specimen Orientation[a] | Energy Absorbed, ft-lb | |
|---|---|---|---|
| | | 72 F | 212 F |
| | Anchor Head HV016 | | |
| 5-1 | L | 11 | - |
| 5-2 | L | 12 | - |
| 5-3 | L | - | 18 |
| 5-4 | L | - | 19 |
| 4-1 | T | 5 | - |
| 4-2 | T | 5.5 | - |
| 4-3 | T | - | 10 |
| 4-4 | T | - | 8.5 |
| | Anchor Head HV038 | | |
| L-1 | L | 15 | - |
| L-2 | L | 13 | - |
| L-3 | L | - | 21 |
| L-4 | L | - | 21 |
| T-1 | T | 7 | - |
| T-2 | T | 7 | - |
| T-3 | T | - | 9.5 |
| T-4 | T | - | 9.5 |

(a) L specimens were parallel to the axis of the cylindrical anchor head. T specimens were parallel to the circular surfaces of the anchor and essentially normal to a diameter.

temperature exhibited 90 to 95 percent brittle fracture. In addition, the transverse specimens tested at 212 F exhibited between 80 and 90 percent brittle fracture; however, the longitudinal specimens tested at 212 F exhibited considerably less brittle fracture, typically only 40 to 50 percent.

## Hardness

Rockwell C hardness measurements were made in essentially radial paths traversing approximately 1-1/2 inches of the 2-inch-wide rim section of Piece 4 from Anchor Head HV016. Those traverses were made on the shim-side surface and on a plane approximately 1 inch from the shim-side surface. Similar Rockwell C hardness traverses were made on Anchor Head HV038 on the shim-side surface, the button-head surface, and on planes approximately 3/4 inch and 1-1/2 inches from the button-head surface. The results of those hardness traverses are listed in the following tabulation:

| Traverse Location | Rockwell C Hardness Range |
|---|---|
| **Anchor Head HV016** | |
| Shim-side surface | 41.5-44 |
| 1 inch from shim-side surface | 41-43 |
| **Anchor Head HV038** | |
| Button-head surface | 43-43.5 |
| 3/4 inch from button-head surface | 41-45 |
| 1-1/2 inch from button-head surface | 39-43 |
| Shim-side surface | 42-44 |

The results of those hardness measurements indicate that the hardnesses of both anchor heads were within the specified range of 40 to 44 Rockwell C. As is noted in the tabulation, for Anchor Head HV038 there was one hardness value (45 $R_c$) that was 1 point above the maximum and one hardness value (39 $R_c$) that was 1 point below the minimum value specified. Those two deviations from the specified range out of 27 measurements are not considered significant with regard to either the failure of these anchor heads or compliance with the specified hardness range.

## Visual Examination

The fracture surfaces on the two pieces (4 and 5) of failed Anchor Head HV016 are shown in Figures 1 and 2, respectively. Those surfaces first were examined visually and with a low-power stereomicroscope. Because of the time constraints to develop the mechanical-property data, that initial examination was performed quickly prior to sectioning the pieces for tensile and impact specimens. That examination indicated that the direction of crack propagation in these sections was from the shim side to the button-head side of the anchor. The fracture surfaces exhibited a primarily brittle appearance. However, a small shear lip was present along the edge of the fractures on the shim side of the anchor. The presence of that shear lip and the absence of other distinguishable markings led to the conclusion that the origin of the failure was not present on the pieces provided for this study. As is shown in Figures 1 and 2, pieces of the steel had fractured from the button-head surfaces; probably in the latter stages of the failure of this anchor head.

The fracture surface on the portion of Anchor Head HV038 provided for study is shown in Figure 3. A distinct fracture origin was not obvious on that surface. However, the general appearance of that surface indicated that the fracture most likely initiated in one or more of the ligaments or webs between the tendon holes in the central region of the anchor head near the shim face. Several of those regions contained no shear lips adjacent to their surfaces and, thus, they were considered to be potential origin sites. The markings on the 2-inch-wide rim portions of the anchor head indicated that those surfaces most likely were formed during the latter stages of the failure of the anchor head. Those fracture surfaces were quite flat and exhibited a woody texture that most likely was related to the nonmetallic inclusions and banding (alloying element segregation) in the steel. Small shear lips were present on the rim fracture surfaces adjacent to the shim-side surface. The presence of those shear lips and the absence of other distinct features of the surfaces of the fracture through the rim regions indicated that the failure did not initiate in those regions.

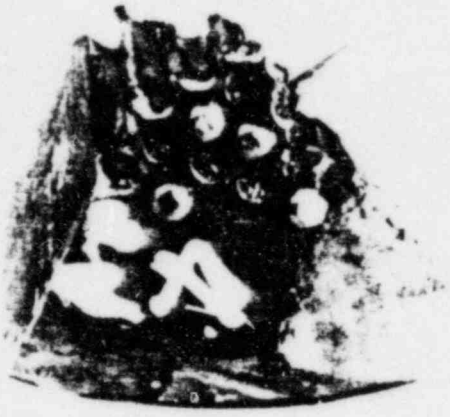

As Received 7317-1

a. Button-Head Surface

As Received 7317-4

b. Fracture Surface on Left Side

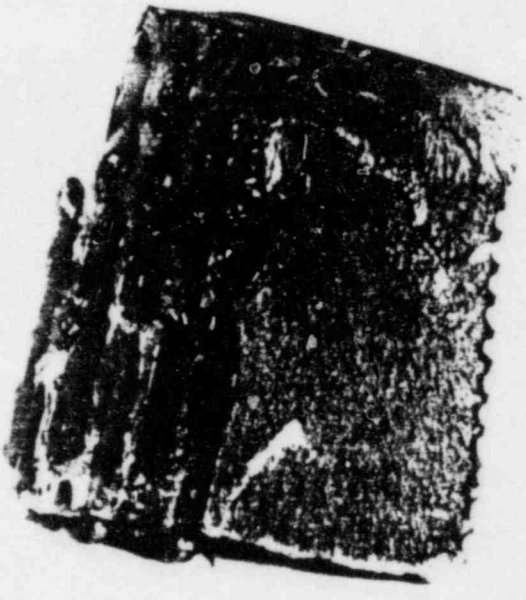

As Received 7317-6

c. Fracture Surface on Right Side

FIGURE 1. PHOTOGRAPHS OF PIECE 4 FROM ANCHOR HEAD HV016

As Received 7317-7

a. Button-Head Surface

As Received 7317-9

b. Fracture Surface on Left Side

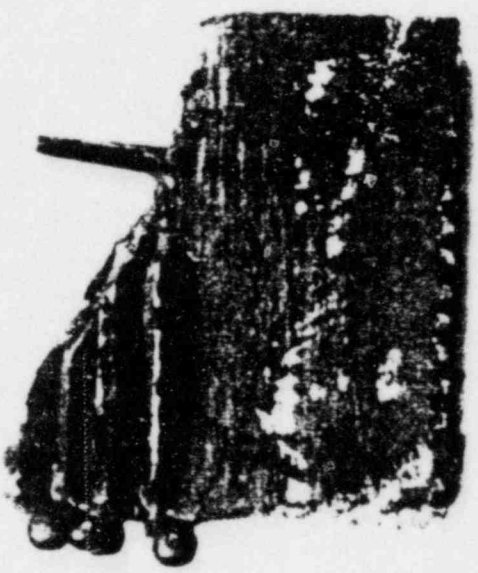

As Received 7317-8

c. Fracture Surface on Right Side

FIGURE 2. PHOTOGRAPHS OF PIECE 5 FROM ANCHOR HEAD HV016


1X

9L828

FIGURE 3. FRACTURE SURFACE OF PIECE FROM ANCHOR HEAD HV038

The button-head surface is at the top of the figure, and the shim-side surface is at the bottom. The portion of the surface contained within the outlined area was examined in the SEM. The arrows point to suspected fracture-origin regions. Circled Regions A and B indicate where SEM fractographs discussed in subsequent sections of this report were taken. Note the white-appearing deposit on the surface of the tendon hole in circled Region C.

No evidence of significant corrosion (rust) was present on the fracture surfaces or on the surfaces of either anchor head. In addition, no evidence was present that would indicate that quench cracks had formed prior to tempering of the anchor heads during their heat treatment. However, some small pits and whitish desposits were present on the surfaces of the tendon holes. One particularly noticeable deposit was located on the surface of a tendon hole in Region C circled on Figure 3.

Examination of the shim-side surfaces of the ligaments between tendon holes revealed the presence of cracks in several of those ligaments in Anchor Head HV038. The locations of those cracks are shown in Figure 4a; Figure 4b shows two of those cracks at higher magnification.

## Scanning-Electron-Microscope Examination

### Anchor Head HV016

The majority of the fractographic examination of the pieces from Anchor Head HV016 in the scanning electron microscope (SEM) was conducted on a fracture surface from Piece 5. That fracture surface is illustrated in Figure 5. The bulk of the other fracture surfaces were destroyed during sectioning to obtain the mechanical-property specimens. The predominant fracture mode observed on the lower portion of the fracture surface shown in Figure 5 was intergranular fracture. Figures 6a and 6b illustrate the predominantly intergranular fracture mode in the regions identified as 5 and 4, respectively, in Figure 5. In Region 3, the fracture mode consisted of a mixture of intergranular fracture and ductile fracture, as is shown in Figure 7. In that region, the intergranular fracture occurred in bands on slightly different planes, and the ductile fracture appeared to result from shear between those bands, forming steps on the fracture surface. In Regions 1 and 2 and the upper portion of the fracture surface shown in Figure 5, the fracture mode consisted of a mixture of ductile and cleavage fracture with varying amounts of cleavage fracture. The typical appearance of the fracture surface in Region 2 is shown in Figure 8, and Figure 9 shows an area of predominantly cleavage fracture in Region 1.

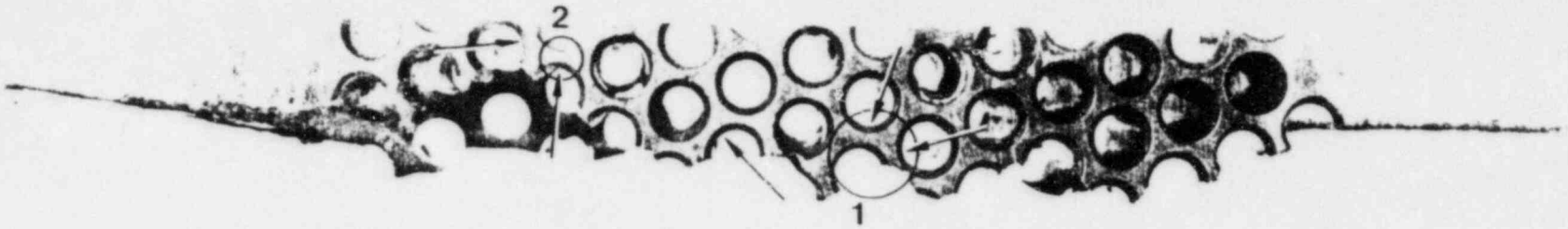


1X

9L829

a. Locations of Cracks Between Tendon Holes. Arrows Indicate Ligaments That Were Cracked; the Crack in Circled Region 2 was Opened to Allow Examination of its Surfaces.

10X

9L827

b. Cracks in Circled Region 1 From (a)

FIGURE 4. PHOTOGRAPHS SHOWING THE LOCATIONS OF CRACKS IN THE LIGAMENTS BETWEEN TENDON HOLES IN ANCHOR HEAD HV038


FIGURE 5. ONE FRACTURE SURFACE ON PIECE 5 FROM ANCHOR HEAD HV016

The numbered regions indicate the locations where SEM fractographs described in subsequent figures were taken.

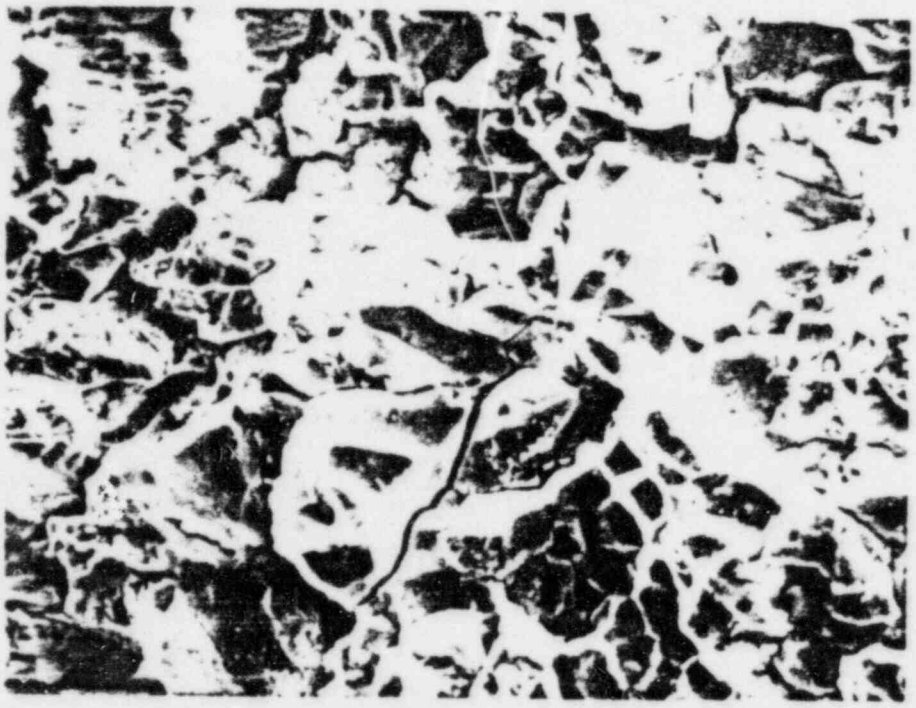

750X

a. Region 5

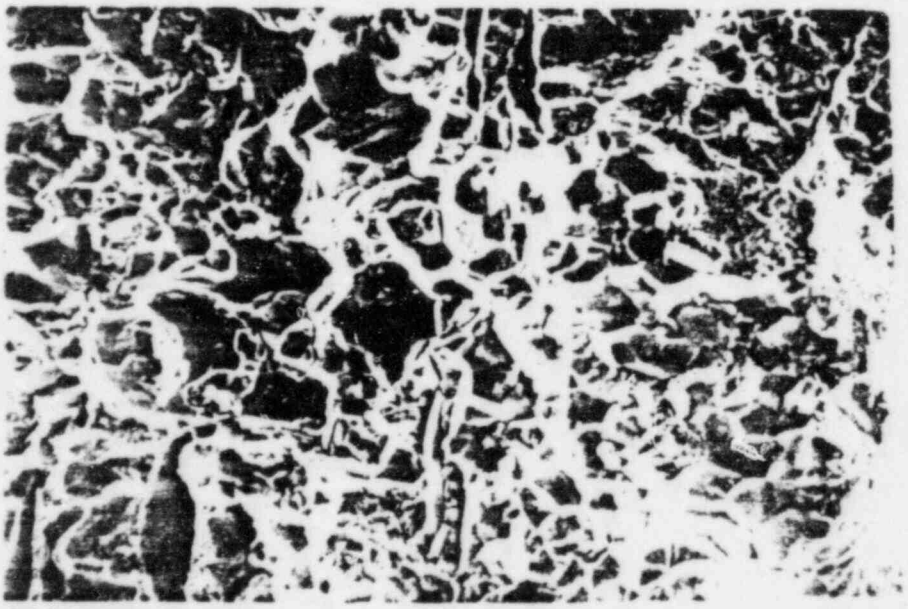

500X

b. Region 1

FIGURE 6. PREDOMINANTLY INTERGRANULAR FRACTURE ON THE LOWER PORTION OF THE FRACTURE SURFACE FROM ANCHOR HEAD HV016 SHOWN IN FIGURE 5

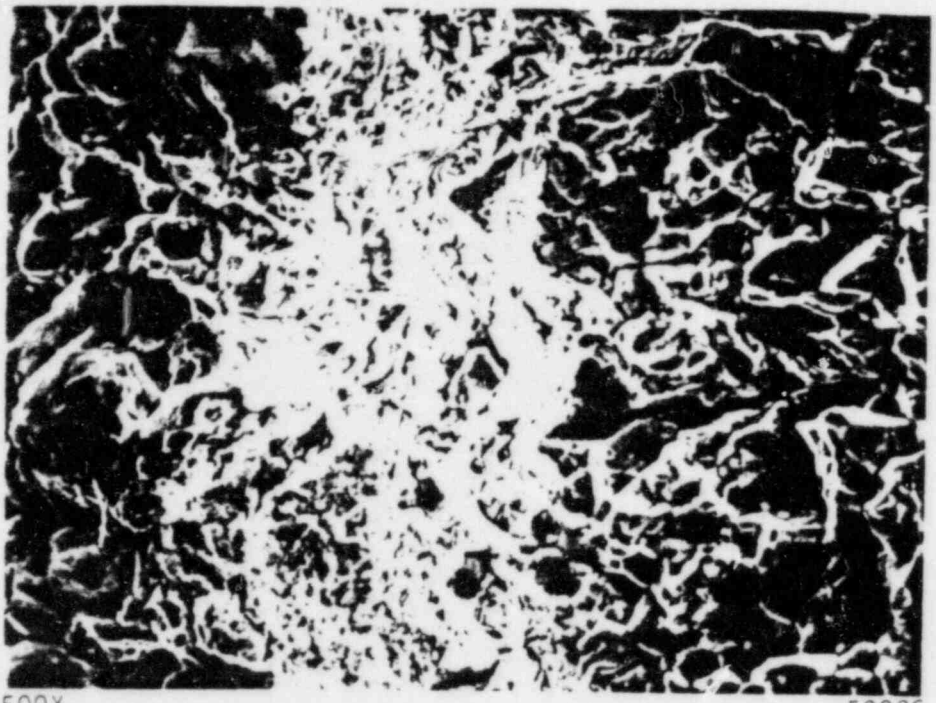


FIGURE 7. BANDS OF INTERGRANULAR FRACTURE AND DUCTILE FRACTURE (SHEAR STEP) OBSERVED IN REGION 3 ON THE FRACTURE SURFACE SHOWN IN FIGURE 5

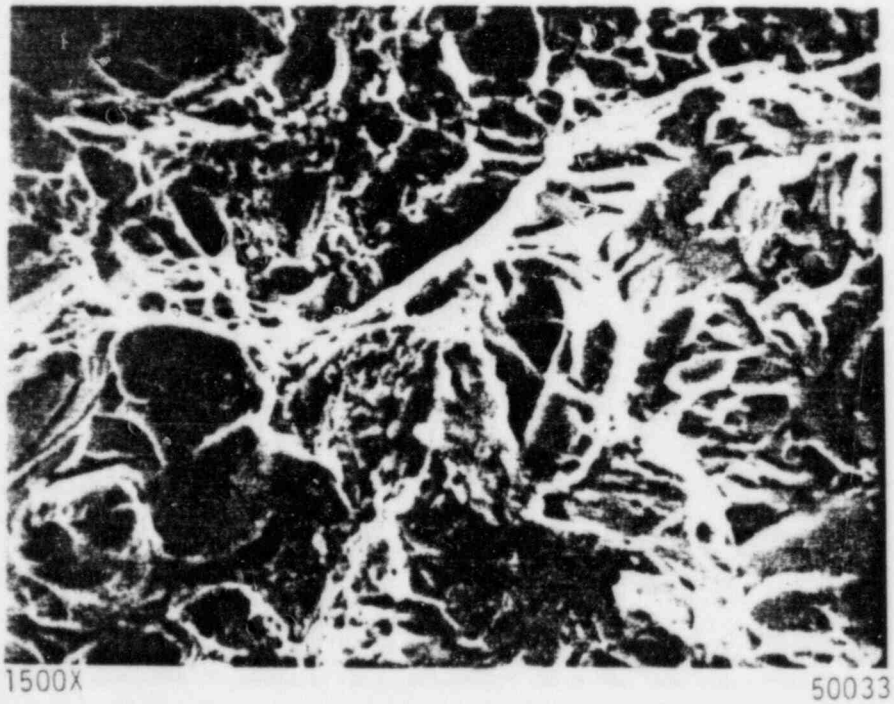


FIGURE 8. MIXTURE OF CLEAVAGE AND DUCTILE FRACTURE OBSERVED IN REGION 2 ON FIGURE 5

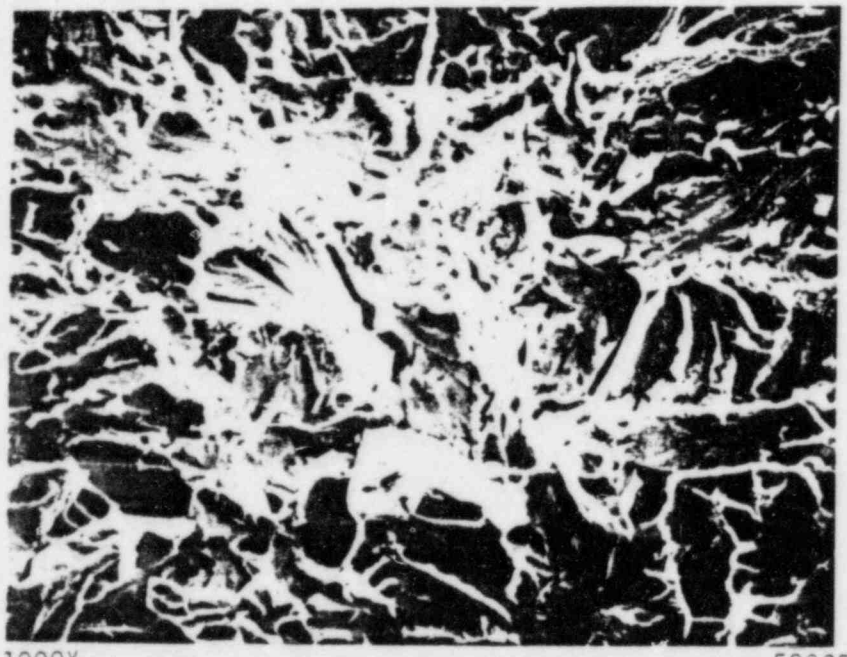

1000X 50035

FIGURE 9. PREDOMINANTLY CLEAVAGE FRACTURE OBSERVED IN REGION 1 ON THE FRACTURE SURFACE SHOWN IN FIGURE 5

All three modes of cracking were observed on the fracture surfaces of the ligaments between the tendon holes. In addition, numerous manganese sulfide inclusion stringers were present on all of the fracture surfaces examined.

Anchor Head HV038

The fractographic examination in the SEM of the fracture surfaces from Anchor Head HV038 was concentrated on the suspected fracture-origin regions illustrated previously in Figure 3. In addition, one of the cracks in the ligaments between the tendon holes was opened so that its surfaces also could be examined (see Figure 4a). Also, a section that contained ligaments between tendon holes from a region where no cracks were apparent was broken in three-point bending in the laboratory, and the surfaces of that freshly produced fracture were examined in the SEM.

Figure 10 illustrates the typical fracture appearance of the suspected fracture-origin regions; that SEM fractograph was taken in Region A shown on Figure 3. As is shown in Figure 10, the fracture surfaces in those regions exhibited predominantly intergranular fracture. Similarly, the predominant fracture mode within the region outlined in Figure 3 was intergranular; however, some regions with mixtures of intergranular and ductile fracture modes also were present in that region as is shown in Figure 11. Figure 11 also shows manganese sulfide inclusion stringers that often were present on the fracture surfaces of many regions examined.

Portions of the fracture surface within the region examined in the SEM exhibited a dark appearance, perhaps indicating the presence of corrosion products. Region B in Figure 3 illustrates that feature. Examination of the surfaces in that region revealed again that the predominant fracture mode was intergranular, as is shown in Figure 12. Energy-dispersive analysis of X-rays (EDAX) in that region revealed the presence of calcium and zinc on the surfaces of that region, in addition to iron, chromium, sulfur, and silicon; the latter four elements were present in the steel. The corrosion-preventative grease contains calcium, and, thus, it

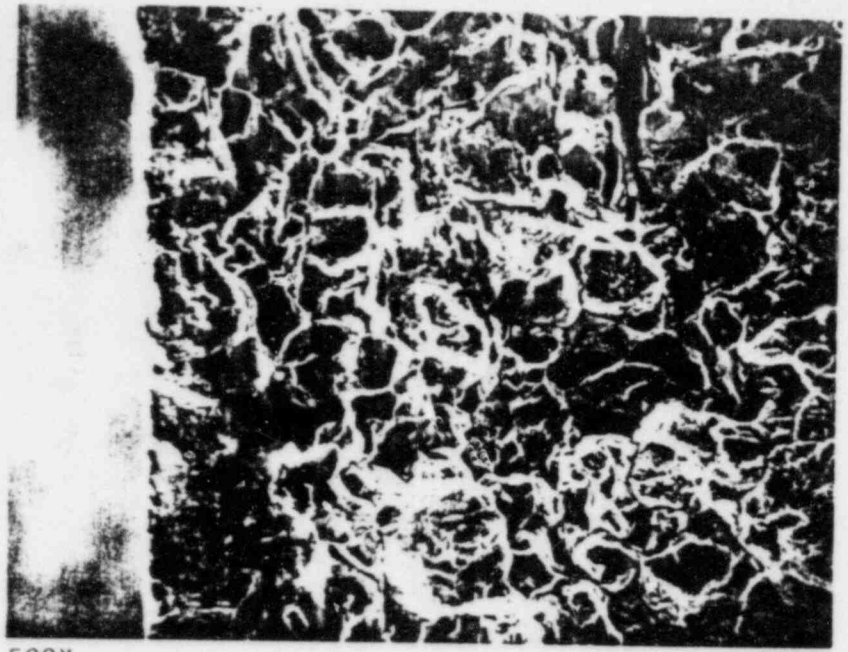

500X 50200

FIGURE 10. TYPICAL INTERGRANULAR FRACTURE OBSERVED AT THE SUSPECTED ORIGIN REGIONS OF THE FRACTURE IN ANCHOR HEAD HV038

The fractograph was taken in Region A shown in Figure 3.

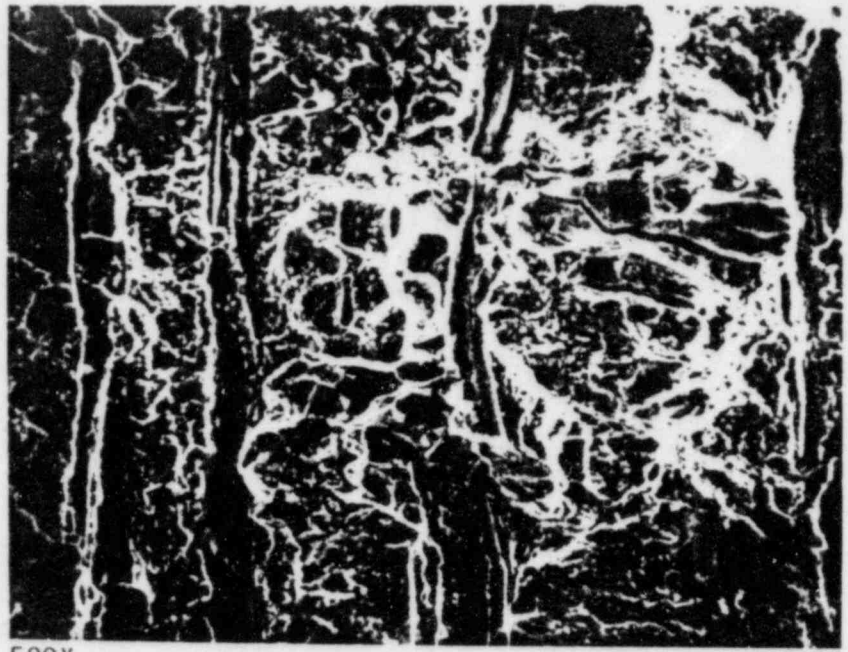

500X 50206

FIGURE 11. MANGANESE SULFIDE INCLUSION STRINGERS AND MIXED FRACTURE MODES ALSO PRESENT IN REGION A IN FIGURE 3

Anchor Head HV038.
The fracture modes present were intergranular and ductile. This fractograph was taken from a region at the right side of the circle labeled A.

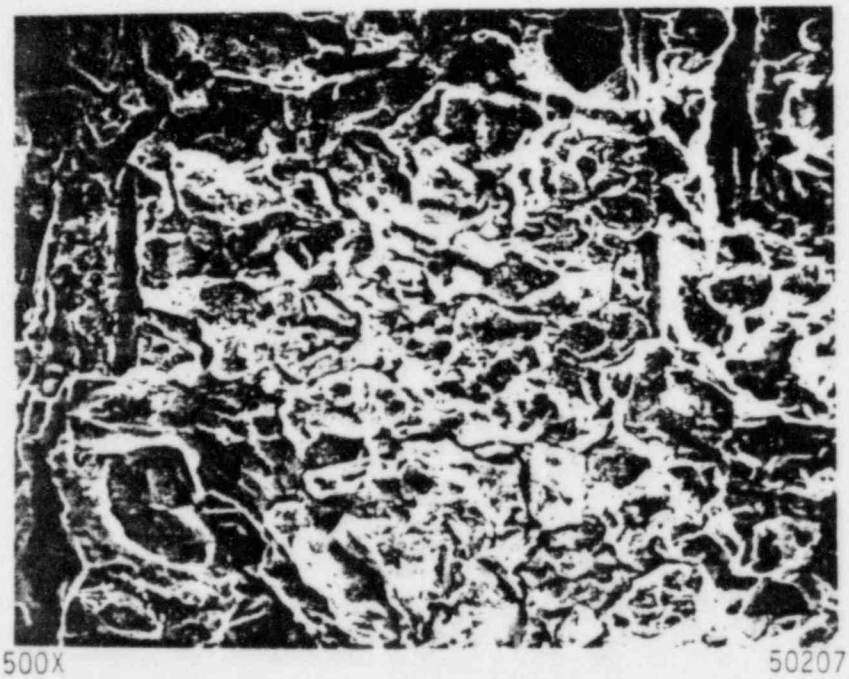


FIGURE 12. TYPICAL INTERGRANULAR FRACTURE IN THE DISCOLORED REGION B IN FIGURE 3

it was presumed to be the source of the calcium detected on the fracture surface. The zinc detected in that region most likely came from corrosion of particles of zinc that may have been transferred to that region when the tendon wires were strung through the galvanized tendon conduit.

Figures 13a and 13b illustrate the appearance of the surfaces of the pre-existing crack in a ligament that was opened in the laboratory. As is shown in Figure 13a, there was a faint thumbnail-shaped region that extended inward from the tendon-hole surface on the left side of the figure, thereby indicating a fracture-origin in that region. As is shown in Figure 13b, the predominant fracture mode adjacent to the tendon-hole surface in that region was intergranular. Toward the tendon surface opposite the origin region, shown in Figure 13a, the fracture surface exhibited a mixture of intergranular and ductile fracture similar to that shown previously in Figure 11.

Figures 14a and 14 illustrate the appearance of the surface of the fracture of a ligament in which no pre-existing crack was present, which was fractured by three-point bending in the laboratory. Figure 14a shows that numerous manganese sulfide inclusion stringers were present, and Figure 14b shows that the fracture mode was a mixture of ductile and cleavage fracture; no intergranular fracture was observed.

## EDAX Analyses of Deposit on Tendon Hole Surfaces

As was shown in Figure 3, circled Region C, there was a white deposit on the surface of one of the tendon holes in Anchor Head HV038. Some of that deposit was collected on a nonmetallic fiber and analyzed by EDAX in the SEM. A similar whitish colored, but much smaller, deposit observed on the surface of a tendon hole in Anchor Head HV016 also was analyzed by EDAX in the SEM along with an adjacent region that did not contain a deposit. Those results of those analyses were as follows:

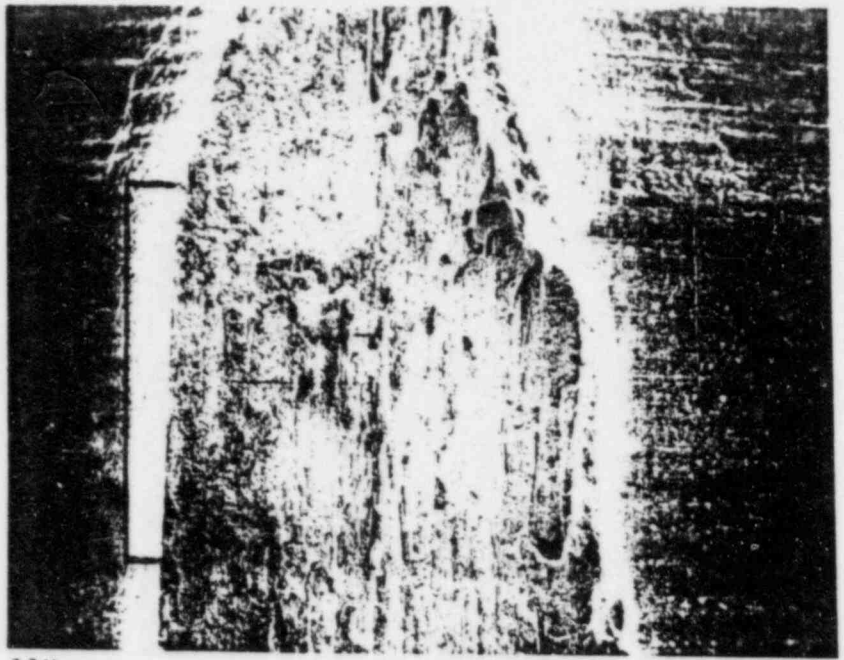

11X 50217

a. General Appearance of Crack Surface Indicating an Origin Adjacent to the Tendon-Hole Surface (Origin Region is Indicated by the Bracket)

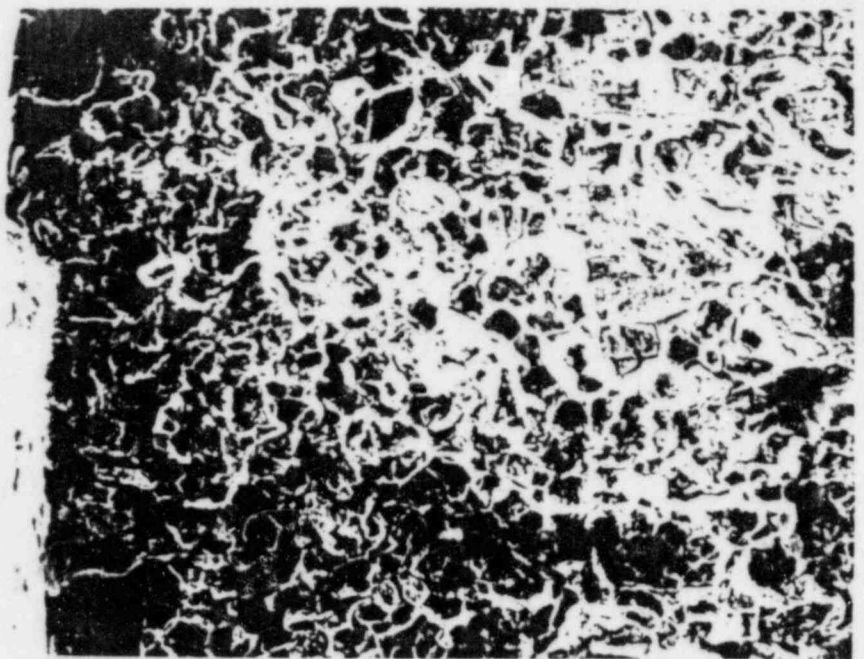

500X 50221

b. Intergranular Fracture Mode at the Origin Region in (a)

FIGURE 13. SURFACE OF THE CRACK IN THE LIGAMENT BETWEEN TENDON HOLES SHOWN IN REGION 2 OF FIGURE 4a THAT WAS OPENED IN THE LABORATORY

100X 50296

a. Typical Fracture Appearance Showing Presence of Numerous Manganese Sulfide Inclusions

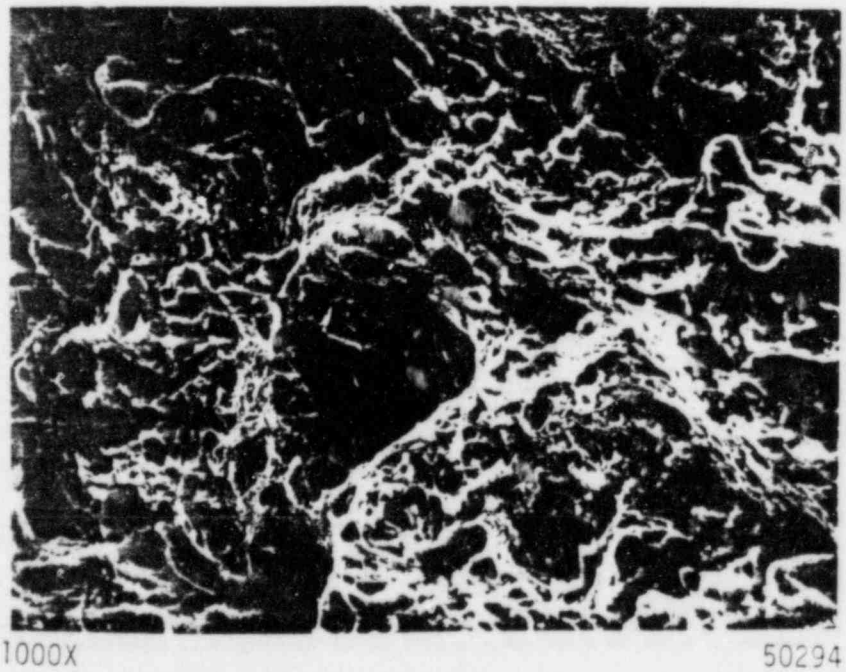

1000X 50294

b. Mixture of Ductile and Cleavage Fracture

FIGURE 14. TYPICAL APPEARANCE OF THE FRACTURE SURFACE OF LIGAMENT BETWEEN TENDON HOLES THAT DID NOT CONTAIN A CRACK AND WAS BROKEN IN THREE-POINT BENDING IN THE LABORATORY

| Identification | Elements Detected, relative weight percent[a] | | | | | | | |
|---|---|---|---|---|---|---|---|---|
| | Zn | Fe | Ca | S | Si | Al | Na | Cr |
| Deposit, HV038 | 3.53 | 8.45 | 60.67 | 9.26 | 4.44 | 5.19 | 8.46 | ND[b] |
| Deposit, HV016 | 4.47 | 86.4 | 2.19 | 1.46 | 2.34 | ND | ND | 2.27 |
| "Clean" Surface, HV016 | ND | 94.8 | ND | 0.30 | 1.09 | ND | ND | 3.06 |

(a) Based on total number of X-ray counts detected.
(b) ND = not detected.

As is shown in the above tabulation, the deposit that was removed from the surface of the tendon hole in Anchor Head HV038 contained a significant amount of Ca (present in the grease), lesser amounts of Fe, S, and Si (present in the steel) as well as Na (present in the grease), Al, and Zn. The zinc presumably was present as an oxide (white rust) and its presence indicates that preferential corrosion of zinc particles entrapped in the tendon holes occurred. The source of the aluminum is not known.

The deposit on the surface of Anchor Head HV016 contained Zn, Fe, Ca, S, Si, and Cr and the adjacent "clean" surface region that did not contain a deposit contained only Fe, Si, Cr, and S. The differences in the relative weight percents of those various elements in the deposit removed from the surface of Anchor Head HV038 with a fiber and the deposit on the surface of Anchor Head HV016 was caused by the electrons penetrating the deposit on HV016 and exciting X-rays from the steel substrate.

## Fracture Surfaces of the Tensile and Impact Specimens From the Anchor Heads

As has been described in the previous sections of this report, the predominant mode of failure of many of the surfaces of the fractures that resulted from the service failures of Anchor Heads HV016 and HV038 was intergranular fracture. That fracture mode suggests: (1) the failures were caused by environmentally induced failed mechanisms, such as hydrogen-stress cracking or stress-corrosion cracking, that are characterized by

intergranular fracture of high-strength steels, and/or (2) the steel was embrittled during processing such that it failed mechanically by intergranular fracture.

The examination of the fracture surfaces produced in the laboratory by three-point loading of a section that did not contain a pre-existing crack indicated that the steel was not embrittled severely during processing. To provide further assessment of whether the anchor heads had been embrittled during processing, the surfaces of the tensile and impact specimens from both anchor heads tested in the laboratory were examined with the SEM to determine the fracture mode. Examination of those fracture surfaces revealed that all of those specimens exhibited mixtures of ductile and cleavage fracture. Examples of those fracture modes were shown previously in Figures 8 and 14b. No intergranular fracture was observed on any of those mechanical-test-specimen fracture surfaces. The absence of intergranular fracture on the mechanical-test specimens indicates that the anchor heads were not embrittled as a result of their chemical composition and/or processing.

## Metallographic Examination

### Microstructure

Two sections for metallographic examination, one longitudinal and one transverse, were prepared from each anchor head. The transverse section from each anchor head traversed the 2-inch-wide solid rim section and intersected several of the tendon-wire holes. Examination of those sections revealed that the microstructures of the steel from both anchor heads consisted of mixtures of tempered martensite and/or bainite with some patches of ferrite in the midregion of the rim. Near the periphery of each anchor head and in the ligaments between the tendon holes, the microstructure consisted essentially of all tempered martensite, as is shown in Figure 15a. With increasing distance from the periphery, more bainite and some patches of ferrite were observed, as is shown in Figure 15b. Slight partial decarburization of the steel was evident at the outer

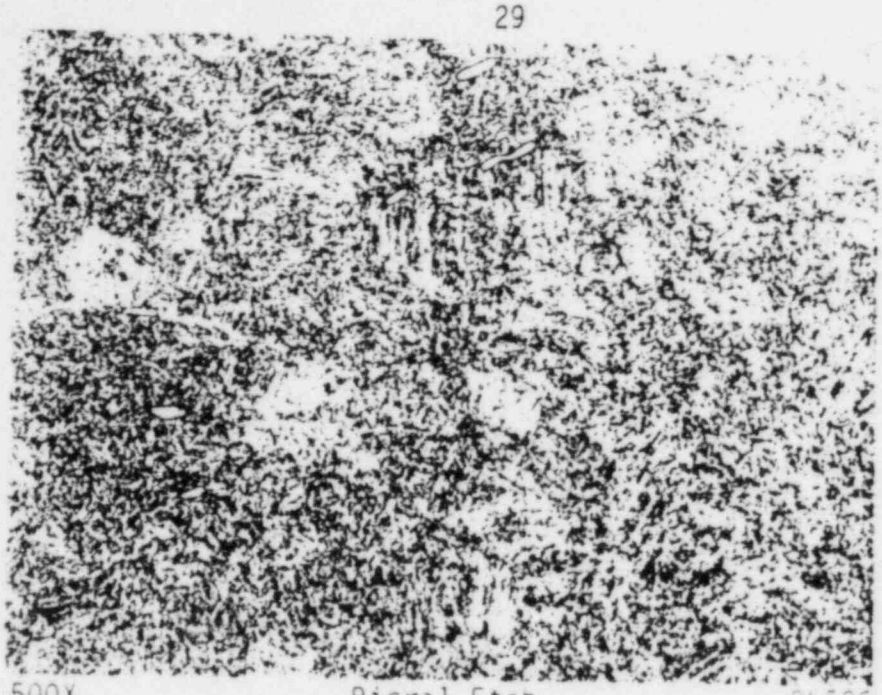

500X Picral Etch 9L505

a. Typical Microstructure Near the Circumferential Surface and Adjacent to the Tendon Holes. The microstructure consists of tempered martensite and/or bainite.

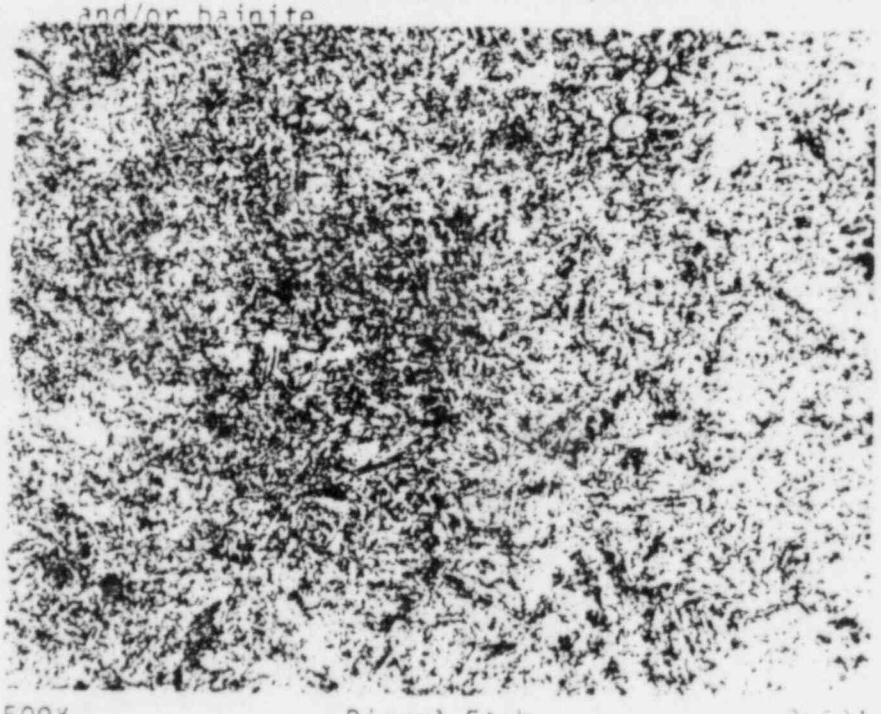

500X Picral Etch 9L504

b. Typical Mixed Microstructure Approximately 1 Inch From the Circumferential Surface of the Anchor Head. It consists of a mixture of tempered martensite and bainite with some small patches of ferrite.

FIGURE 15. TYPICAL MICROSTRUCTURES OF THE STEEL FROM ANCHOR HEADS HV016 AND HV038

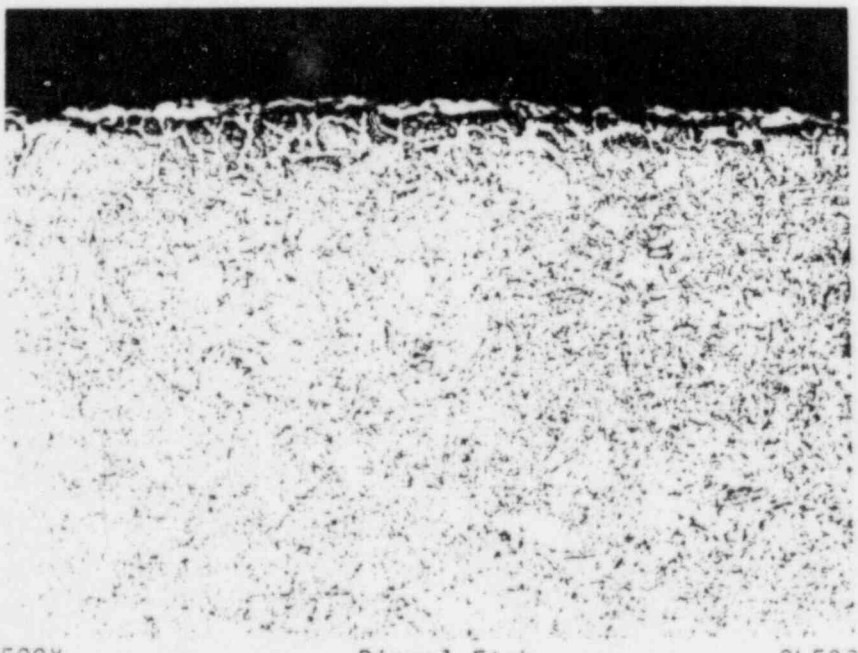

500X Picral Etch 9L508

c. Partial Decarburization at the Circumferential Surface of the Anchor Head

FIGURE 15. (Continued)

surface of the anchor heads and at the surfaces of the tendon holes. That partial decarburization is shown in Figure 15c; the light-etching patches of ferrite that extended inward from the surface to a depth of about 0.001 inch indicate the partial decarburization.

## Cleanliness Ratings

The cleanliness of the steels was rated on the longitudinal sections from the two anchor heads in accordance with the procedures in ASTM E45, Method A. The results are listed in the following tabulation:

| | Cleanliness Rating | | | |
|---|---|---|---|---|
| Identification | Type A (Sulfides) | Type B (Silicates) | Type C (Alumina) | Type D (Globular Oxides) |
| HV016 | 4H | 2H | -- | 1H |
| HV038 | 4H | -- | 3H | 3H |

Those results indicate that the steels from both anchor heads were relatively dirty with respect to the Type A (sulfide) inclusions. In addition, the section examined from Anchor Head HV038 was somewhat dirty with respect to Type C (alumina or aluminates) and Type D (globular oxide inclusions).

## Examination of Failed Tendon Wires

The sections of failed Anchor Head HV016 provided to Battelle for this study, contained portions of eight failed tendon wires. It was mutually decided among representatives of INRYCO, Inland Steel Company, and Battelle to examine the fracture surfaces of those wires to determine if they failed in a brittle manner. The surfaces of all eight tendon wires were examined visually and with a low-power stereomicroscope. The regions adjacent to all the fractures showed evidence of necking, and all the fractures appeared to be the result of overstress. Subsequently, the fracture surfaces on three of those wires were examined in the SEM.

Figure 16 illustrates the typical appearance of the fractures in the tendon wires at low magnification and shows the very apparent necking of the wire prior to rupture. Examination of the fracture surfaces of the three tendon wires at higher magnifications revealed that the fracture modes present were ductile and cleavage fracture. Figure 16b illustrates a mixture of ductile and cleavage fracture in Region A of Figure 16a, and Figure 16c illustrates predominantly ductile fracture in Region B of Figure 16a. These observations suggest that the tendon wires examined failed by overstress, most likely as a result of the changes in stress distribution when the anchor head failed, rather than prior to the failure of the anchor head. However, only a limited number of tendon wire fractures were available for examination. On the other hand, none of the tendon wires that passed through cracked Anchor Head HV038 reportedly had failed. That observation suggests that the anchor heads fail prior to failure of the tendon wires.

## DISCUSSION OF RESULTS

The results obtained from the metallurgical evaluation of the pieces of Anchor Head HV016 have shown that the steel met the chemical-composition requirements for ASTM A3222, Grade 4140/4142, steel in all respects. The average carbon content from the piece of Anchor Head HV038 examined was found to be 0.48, whereas the maximum allowable carbon content for a product analysis is 0.47 percent. However, it is not likely that the slightly higher carbon content of the steel from Anchor Head HV038 had a significant effect on the failure. The sulfur contents of the steels from both anchor heads were relatively high, but well within the specification limits, and both anchor heads contained numerous manganese sulfide inclusion stringers. The contents of the nonspecified residual elements that can promote brittleness of steel under appropriate processing or testing conditions were low and, thus, most likely those elements did not contribute to these failures.

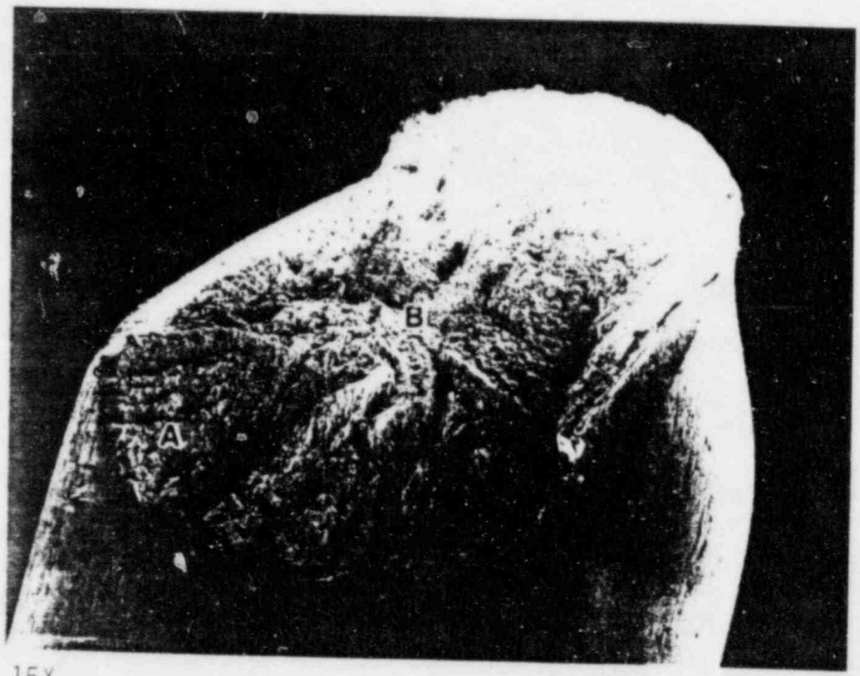


15X 50155

a. General Appearance of Failed Tendon Wire

FIGURE 16. TYPICAL APPEARANCE OF THE FRACTURES OF THE TENDON WIRES EXAMINED

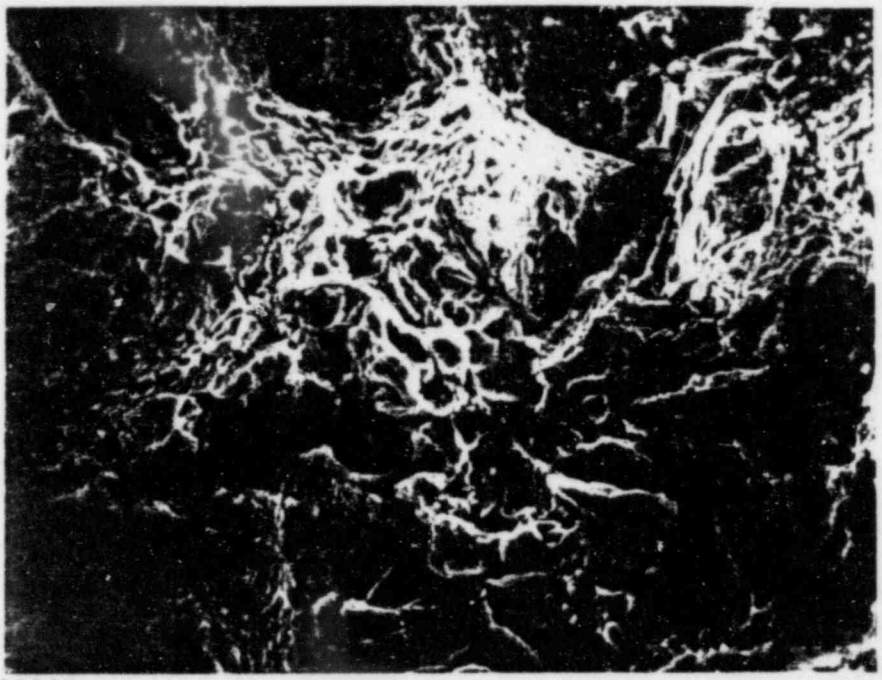

1000X 50164

b. Ductile and Cleavage Fracture in Region A in Figure 15a

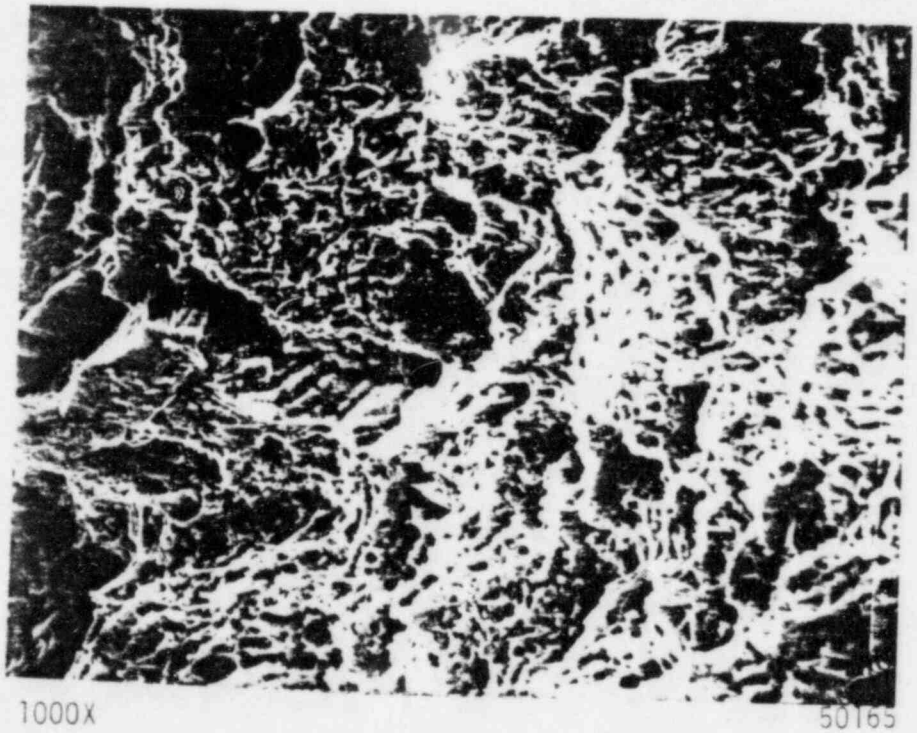

1000X 50165

c. Predominantly Ductile Fracture in Region B in Figure 15a

FIGURE 16. (Continued)

The hardness of the steel from Anchor Head HV016 ranged from 41 to 44 Rockwell C and, thus, was within the specified range of 40 to 44 Rockwell C. The hardnesses measured on various sections from Anchor Head HV038 ranged from 39 to 45 Rockwell C and averaged 42.5 Rc. Of the 27 hardness readings, there was one at 39 Rc and one at 45 Rc; all of the others were within the specified range of 40 to 44 Rc. The hardnesses measured on the button head and the shim-side surfaces ranged from 42 to 44 Rockwell C.

The ultimate tensile strengths of the steel from both anchor heads were consistent with the hardnesses, and there was relatively little difference in the average strength properties of the specimens from the two anchor heads or with respect to specimen orientation. In addition, the ductilities and impact properties of the steel from the two anchor heads were similar. The ductilities and impact properties were significantly lower for the transverse specimens from both anchors heads than for the longitudinal specimens. The differences in those properties with respect to specimen orientation are not unusual for wrought low-alloy engineering steels heat treated to the strength of the anchor heads. At least part of the lower ductility and toughness of the transverse specimens can be attributed to the relatively high sulfur contents and the presence of the manganese sulfide inclusion stringers.

The examination of the fracture surfaces produced during the failures of both anchor heads during service revealed the presence of considerable amounts of intergranular fracture. That fracture mode was present on the surfaces of the fractures in the ligaments between the tendon holes as well as in various regions of the 2-inch-thick rim section. In addition, that fracture mode was present on the surfaces of the pieces that appeared to have spalled off the button-head surface of Anchor Head HV016. In other regions of the field failures, the fracture mode consisted of mixtures of ductile and cleavage fracture modes. Intergranular and cleavage fracture modes are characteristics of brittle fracture. Cleavage fracture usually indicates that fracture occurred at a temperature below the ductile-to-brittle fracture-transition

temperature of the steel. Cleavage fracture also can occur under complex loading conditions that lead to biaxial or triaxial stresses in the part. Analysis of the service loading conditions of an anchor head has shown that complex loading does exist.* In addition, examination of fracture surfaces on the impact specimens from both anchor heads tested at room temperature and 212 F revealed that cleavage fracture was present on the specimens. For those reasons, regions of cleavage fracture would be expected on the service failures.

The presence of intergranular fracture, however indicates that the steel was embrittled either from a combination of its composition and processing or as the result of interactions between the steel and the service environment. Embrittlement mechanisms that cause intergranular fracture that result from the combination of steel composition and processing include temper embrittlement and "500 F", or tempered-martensite, embrittlement. In addition, the formation of grain-boundary sulfide films during the processing of the steel can result in intergranular fracture. Descriptions of those embrittlement mechanisms obtained from the Metals Handbook** are as follows:

> Temper Embrittlement. Embrittlement that results in steels that have been heated in the temperature range. Temper embrittlement usually is detected by an upward shift in the ductile-to-brittle transition temperature in a notched-bar test, such as a Charpy V-notch impact test. The tensile properties of the steel generally are not influenced by this embrittlement mechanism, except in cases of extreme embrittlement. It is caused by the segregation of impurity elements (phosphorus, arsenic, tin, antimony, and possibly others) to the prior-austenite grain boundaries.

---

* Pecknold, D. A., and Presswalla, H. H., "Elastoplastic Analysis of Thick Perforated Plates With Application to Prestressing Anchor Heads", Computers & Structures, 17 (4), 539-553 (1983).

** Metals Handbook, 9th Ed., Volume 1, Properties and Selection: Irons and Steels, B. P. Bardes, Editor, American Society for Metals, Metals Park, Ohio (1978), pp 684-685.

500 F Embrittlement. Occurs when steels with tempered-martensite and/or lower bainite microstructures are tempered in the temperature range from approximately 400 to 700 F. It is detected by measuring the effect of tempering temperature on room-temperature impact energy; this is in contrast to temper embrittlement, which is evaluated by measuring the effect of tempering temperature on the ductile-to-brittle fracture-transition temperature. 500 F embrittlement is believed to be caused by ferrite networks resulting from precipitation of cementite platelets along prior austenite grain boundaries. However, some investigators believe that the precipitation of grain-boundary cementite platelets as such is responsible for 500 F embrittlement.

The low levels of residual elements that promote temper embrittlement present in the two-anchor heads and the absence of intergranular fracture on the surfaces of the tensile specimens and the impact specimens tested in the laboratory strongly indicates that neither temper embrittlement nor 500 F embrittlement were responsible for the intergranular fracture observed on the fracture surfaces of these anchor heads.

Failure mechanisms that involve interaction of a high-strength steel part and its environment that can result in intergranular fracture are hydrogen-stress cracking (HSC) and stress-corrosion cracking (SCC). Both of these failure mechanisms are time dependent and, thus, appear to be more consistent with the fact that the anchor failed some time after 6 years of service. Stress-corrosion cracking can occur without significant general corrosion; however, usually when SCC occurs some corrosion products are present on the surface of the part or on the fracture surfaces of the part. No significant corrosion products were detected on the fracture surfaces of the pieces from either anchor head examined at BCL.

Hydrogen-stress cracking, also referred to as hydrogen-induced, delayed, brittle failure, is a cracking mechanism that results in a brittle fracture in nominally ductile steel at applied tensile stresses below the yield strength while the steel is subjected to a sustained load. Steels with hardnesses below about 20 Rockwell C are essentially immune to hydrogen-

stress cracking, but with increasing hardness above 20 $R_c$ the susceptibilities of the steels to hydrogen-stress cracking increases. The applied stress level that will result in hydrogen-stress cracking varies inversely with the strength level of the steel; that is as the strength level (hardness) increases, the threshold applied stress decreases. For this failure mechanism to be operative, the steel must contain atomic hydrogen from processing or absorb-hydrogen from its service environment. The amount of hydrogen required to cause cracking is dependent upon the strength level of the steel and the applied stress level. The higher the strength level and the applied stress level, the lower the hydrogen content or hydrogen charging rate from the environment required for cracking. If the conditions for hydrogen-stress cracking are satisfied, failures will occur after some period of time during which cracks nucleate and grow to critical size. The time for failure to occur is related to the strength level, applied stress level, and the hydrogen content or severity of the environment. At high values of those three factors, failure can occur in very short times such as minutes or hours. At low values of one or more of those factors, the time for failure may be years.

The anchor head satisfies two of the conditions for hydrogen-stress cracking: high-strength steel that is subjected to sustained tensile stresses. It was reported by other investigators working on the failure of Anchor Head HV016 that water that contained chlorides and other ionic species was detected in the grease from the grease can surrounding the anchor heads. Also, it was reported that the concentrations of certain ionic species in the grease were higher than the specified amounts. However, there is some question as to whether the grease was contaminated during or after removal of the grease can. Subsequently, water was found in the grease from the can surrounding Anchor Head HV038. Thus, it is possible to have a potential source of atomic hydrogen in the vicinity of the anchor head. That source of hydrogen would be corrosion of the steel in the water. Furthermore, small corrosion pits and deposits were observed on the surfaces of some of the tendon holes in the pieces from Anchor Heads HV016 and HV038 examined at Battelle. EDAX analysis revealed the presence of calcium and zinc in those deposits. Silicon, chromium, iron, and nickel also were detected in those deposits, however, those elements are present in the steel

and may have been detected because X-rays penetrated the deposits. The grease reportedly contains significant amounts of calcium and, thus, the calcium detected most likely came from it. The zinc may have been washed into that region by water, or small flakes of zinc may have been picked off by the tendon wires when they were threaded through the galvanized conduit when the posttensioning system was installed. Since zinc is anodic to steel, local galvanic corrosion between the zinc and the steel may have resulted in atomic hydrogen being deposited on the steel. Some of that hydrogen may have entered the steel and caused cracks to initiate and grow by hydrogen-stress cracking. Such a cracking mechanism would result in intergranular fracture in the regions where the hydrogen-stress cracks were growing. Once the cracks reached a critical size, the remaining section would fail rapidly and, most likely, in these anchor heads the regions of fast fracture would exhibit cleavage and/or ductile fracture modes. Furthermore, hydrogen-stress cracking is a time-dependent failure mechanism. That is, time is required for the cracks to initiate and grow. Also, it may have taken time for the conditions that allowed water to be present in the anchor-head region to develop. Those time-related factors are consistent with the fact that the failure occurred some time after 6 years of service. Thus, based upon the information obtained from the studies of the failures of Anchor Head HV016 and HV038, it appears that hydrogen-stress cracking is the most probable cause of failure.

To prevent similar failures of anchor heads processed to this hardness range in the future, methods must be employed to prevent water from contacting the surfaces of the anchor heads. Those steps should include thoroughly coating the anchor-head surfaces with corrosion-prevention grease and eliminating the source(s) of water in the post-tensioning system. In addition, the design of the posttensioning system should be reviewed and considerations given to modifications to permit the anchor heads to be made of a lower strength steel that will be less susceptible to hydrogen-stress cracking and other environmentally induced failure mechanisms.